Charge transport through O-deficient Au-MgO-Au junctions

M. M. Fadlallah,[1,2] C. Schuster,[1] U. Schwingenschlögl,[3] I. Rungger,[4] and U. Eckern[1]
[1]*Institut für Physik, Universität Augsburg, 86135 Augsburg, Germany*
[2]*Physics Department, Benha University, Benha, Egypt*
[3]*KAUST, PSE Division, Thuwal 23955-6900, Kingdom of Saudi Arabia*
[4]*School of Physics and CRANN, Trinity College, Dublin 2, Ireland*
(Received 10 September 2009; revised manuscript received 22 October 2009; published 29 December 2009)

Metal-oxide heterostructures have been attracting considerable attention in recent years due to various technological applications. We present results of electronic structure and transport calculations for the Au-MgO-Au (metal-insulator-metal) heterostructure based on density-functional theory and the nonequilibrium Green's functions method. The dependence of the conductance of the heterostructure on the thickness of the MgO interlayer and the interface spacing is studied. In addition, we address the effects of O vacancies. We observe deviations from an exponentially suppressed conductance with growing interlayer thickness caused by Au-O chemical bonds. Electronic states tracing back to O vacancies can increase the conductance. Furthermore, this effect can be enhanced by enlarging the interface spacing as the vacancy induced Mg states are shifted toward the Fermi energy.

DOI: 10.1103/PhysRevB.80.235332 PACS number(s): 73.20.−r, 73.40.Rw

I. INTRODUCTION

Metal-oxide heterostructures are most important for many areas of science and engineering such as structural materials, photovoltaic devices, heterogeneous catalysis, coatings and sensors.[1] Their properties are often dominated by the interfaces between the component materials, which can show electronic features not present in the bulk systems. For example, conduction states may be created at the interface between two insulating compounds[2] or charge-transfer effects may perturb the electronic structure.[3] Various heterointerfaces between a metal and an insulator, typically metal-oxide interfaces, have been studied.[4–11]

Beyond, tunnel junctions with ferromagnetic metals are of utmost importance in spintronics.[12] The Fe-MgO-Fe heterostructure often is considered a prototypical magnetic tunnel junction for spintronics applications and therefore has been subject to intensive experimental and theoretical research, see Ref. 13, and the references therein. From the experimental point of view, significant progress has been achieved in the determination of the atomic structure of ceramic-metal interfaces, in particular by high-resolution electron microscopy[14] and atom probe field ion microscopy.[15] Furthermore, spatially resolved electron energy loss spectroscopy is able to elucidate the electronic structure of ceramic-metal interfaces.[16] The Au-MgO interface has been described in detail in Ref. 17. The interface configurations in Pd-MgO have been compared in Ref. 18 with respect to the energetic position of the electronic states.

Point defects occur naturally and by design in insulating and semiconducting crystals, producing characteristic optical and electronic properties.[19] In the following we focus on defects due to vacancies. In MgO, the latter are classified as F (color) centers when an O atom is removed and V centers when an Mg atom is removed. O and Mg vacancies appear not only in MgO bulk crystals[20] but especially accumulate at interfaces. Experimentally, vacancies have been found on the surfaces of Au nanoparticles embedded in MgO (Ref. 21) and defects have been observed on the [001] surface of ultrahigh vacuum cleaved single MgO crystals.[22] In addition, bonding between metal atoms and defects has been reported for both the Au-MgO (Ref. 23) and the Fe-MgO (Ref. 24) heterointerface.

In this context, the Au-$(MgO)_n$-Au heterostructure, where the parameter n denotes the thickness of the MgO interlayer in unit cells, is a prototypical system for investigating the influence of structural defects. For interfaces with O and Mg atoms adjacent to the Au atoms, respectively, we will discuss the dependence of the transport properties on n and the interface spacing. In addition, we will study in detail the effects of O vacancies incorporated into the heterostructure. To achieve this goal, we employ the SIESTA (Ref. 25) and SMEAGOL (Refs. 26 and 27) simulation packages. Our paper is organized as follows: after describing the computa-

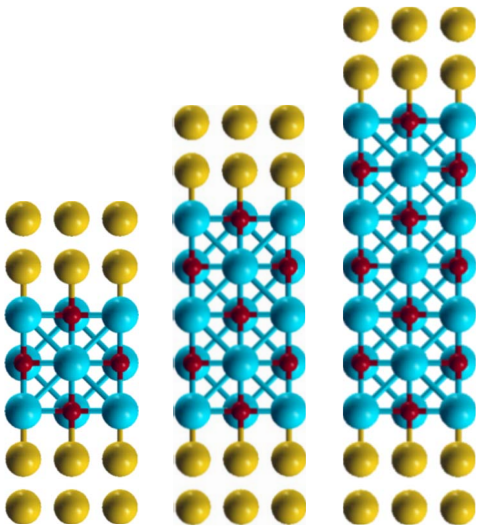

FIG. 1. (Color online) Heterostructures under investigation (from left to right): $n=1,2,3$ unit cells of MgO sandwiched between Au leads. Interface conf. I is shown, see the text for details.

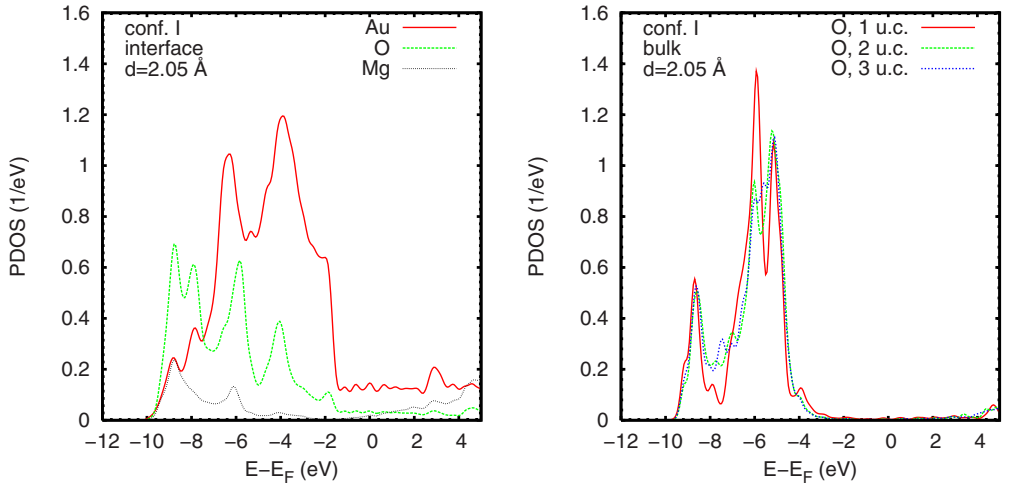

FIG. 2. (Color online) Projected DOS of atoms at the interface for $n=1$ (left-hand side) and of O atoms in the center of the MgO interlayer for $n=1,2,3$ (right-hand side).

tional method and settings in Sec. II we will present in Sec. III electronic structure and transport results for clean Au-MgO-Au junctions without vacancies. In Sec. IV we then will focus on the effects of F centers in the MgO interlayer. In Sec. V we will present our conclusions.

II. COMPUTATIONAL METHOD AND SETTINGS

We construct the Au-MgO-Au supercell by sandwiching an MgO layer of $n=1$, 2, or 3 fcc MgO unit cells, i.e., 3, 5, or 7 MgO monolayers, between two semi-infinite double layer fcc Au [100] electrodes. For establishing the transport properties we consider two configurations of the Au-MgO-Au junction: Either the interface Au atoms lie on top of O (conf. I, shown in Fig. 1) or on top of Mg (conf. II). It has been demonstrated earlier that conf. I is lower in energy.[17] The junctions are assumed to be periodic in the xy plane with z being the transport direction. As a consequence of the 3% lattice mismatch between Au and MgO we have to introduce a minor lattice strain by setting the MgO lattice constant to the Au value $a_{\mathrm{Au}}=4.09$ Å instead of $a_{\mathrm{MgO}}=4.2$ Å. It can be assumed that this lattice strain does not affect our conclusions, as the forces parallel to the interface are moderate. For the Au-MgO distance, i.e., the interface spacing, we study values of $d=2.05$, 2.5, and 3.06 Å.

The SMEAGOL package is based on density function theory, using SIESTA, and the nonequilibrium Green's functions method. Recently it has been used to describe the transport through rough Al, Cu, Ag, and Au interfaces[28] and the Fe-MgO-Fe heterostructure.[13] We apply norm-conserving pseudopotentials in the fully nonlocal Kleinman-Bylander form[29] with a single zeta basis set and, analogous with related studies,[30] the local density approximation. A mesh of $15\times15\times100$ k points is employed in the leads calculation, while a mesh of $10\times10\times1$ k points is used to evaluate the transmission coefficient and the current at different bias voltages. To determine the density matrix, we choose 16 energy points on the real axis and likewise 16 points on both the semicircle and the line in the complex plane. Moreover, 16 poles in the Fermi distribution are employed. We have thoroughly checked the electronic structure results of bulk MgO and Au by comparing them to data from previous studies. In

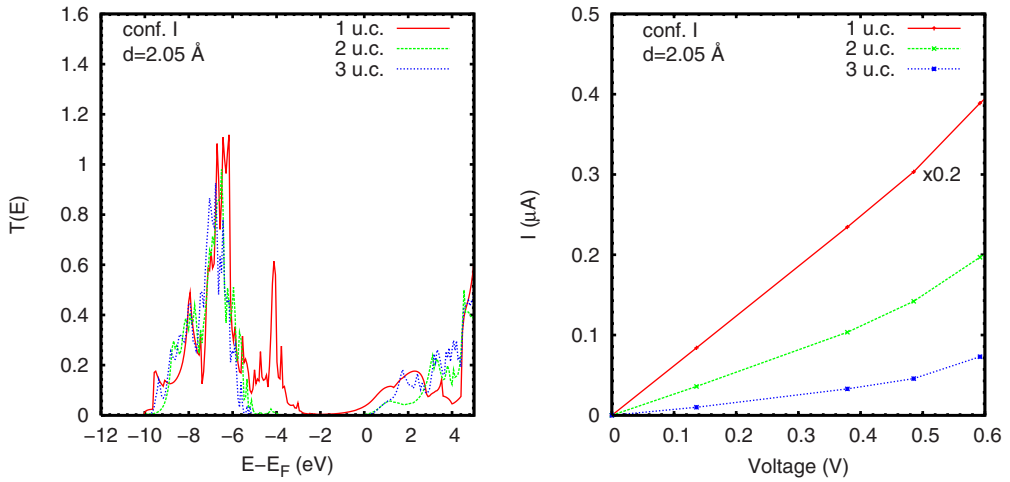

FIG. 3. (Color online) Transmission coefficient (left-hand side) and I-V characteristic (right-hand side) for $n=1,2,3$.

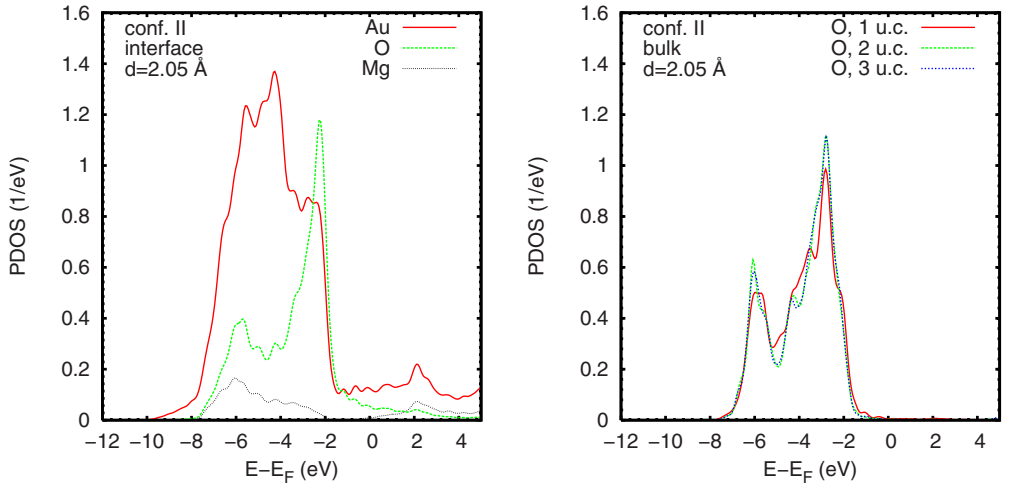

FIG. 4. (Color online) Projected DOS of atoms at the interface for $n=1$ (left-hand side) and of O atoms in the center of the MgO interlayer for $n=1,2,3$ (right-hand side).

particular, the band gap of MgO is found to be 5.16 eV, which agrees well with the theoretical values reported in Refs. 31 and 32, but is lower than the experimental value of 7.8 eV (Ref. 33) due to the underestimation of band gaps by the local density approximation.

III. CHARGE TRANSPORT THROUGH THE CLEAN JUNCTION

We first study the electronic structure of conf. I at an interface spacing of $d=2.05$ Å. To this aim, we analyze the projected density of states (PDOS), see Fig. 2. On the left-hand side, the PDOS of atoms right at the interface is plotted for the $n=1$ system. A strong hybridization between the Au and MgO states is evident. As compared to bulk MgO, additional interface states are found near the lower MgO band edge at −8 eV and at −4 eV.[34] Thus, formation of an interface Au-O bond is evident. Au induced gap states fill up the MgO band gap and leave the interface metallic. The PDOS calculated for O and Mg atoms in the center of the interlayer turns out to be bulk-like even for the thin $n=1$ interlayer, see the right-hand side of Fig. 2. The occupied states in the energy range between −10 and −2 eV are O $2p$ dominated, whereas the Mg $3s$ states dominate at higher energy. When the thickness of the MgO layer increases to $n=2$ the peaks at −8 and −4 eV, reminiscent of the Au-O bonding, vanish. While distinct differences are visible in the PDOS of the central MgO layer for $n=1$ and $n=2$, the result for $n=3$ largely resembles the $n=2$ PDOS.

Corresponding transport data are shown in Fig. 3. For low energies of −10 to −6 eV the shape of the transmission coefficient as a function of the energy, $T(E)$, is closely related to the PDOS of the central MgO layer, see the right-hand side of Fig. 2. However, the transmission vanishes at about −5.5 eV although there is a significant PDOS up to −4 eV for all systems under investigation. Only for the $n=1$ interlayer transmission is found up to about −3 eV, where the transmission peak at −4 eV is related to the interface states. The Au induced gap states lead to a remarkable transmission at the Fermi energy in the $n=1$ case. Since they cannot pen-

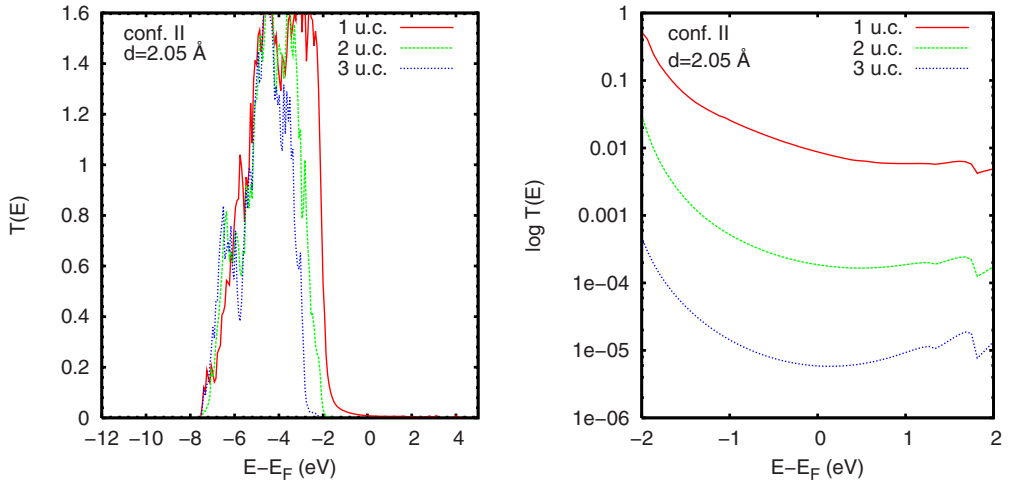

FIG. 5. (Color online) Transmission coefficient for $n=1,2,3$. Logarithmic plot of the data in a reduced energy range is shown on the right-hand side.

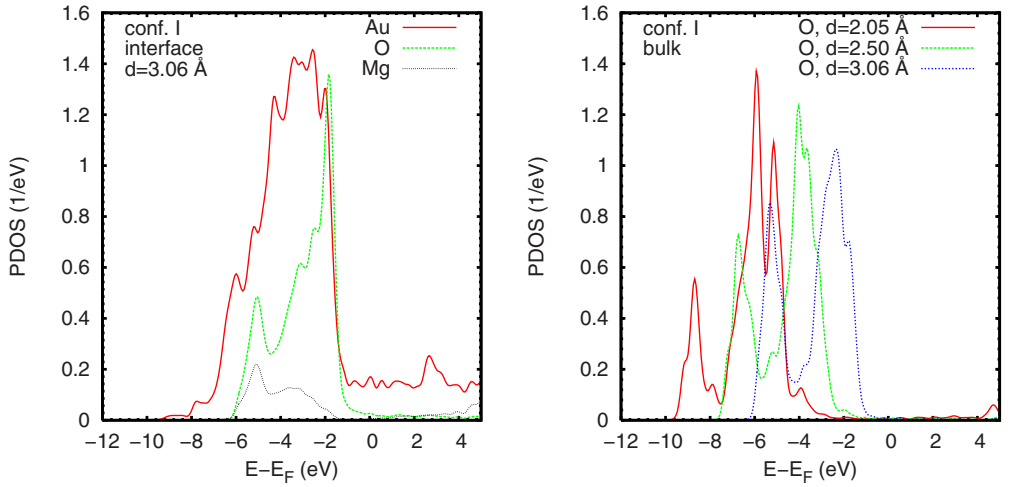

FIG. 6. (Color online) Projected DOS of atoms at the interface at $d=3.06$ Å for $n=1$ (left-hand side) and of O atoms in the center of the MgO interlayer at different values of the interface spacing for $n=1$ (right-hand side).

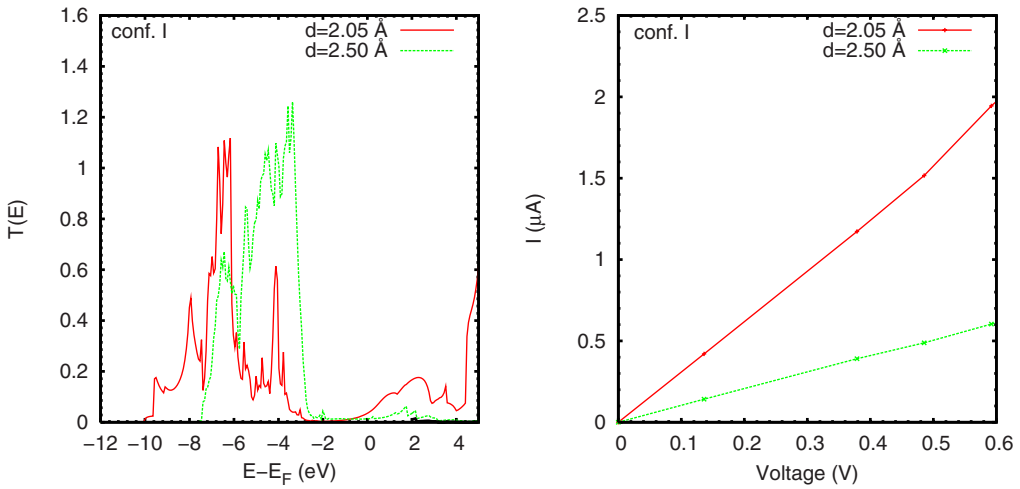

FIG. 7. (Color online) Transmission coefficient (left-hand side) and I-V characteristic (right-hand side) at interface spacings of 2.05 Å and 2.50 Å for $n=1$.

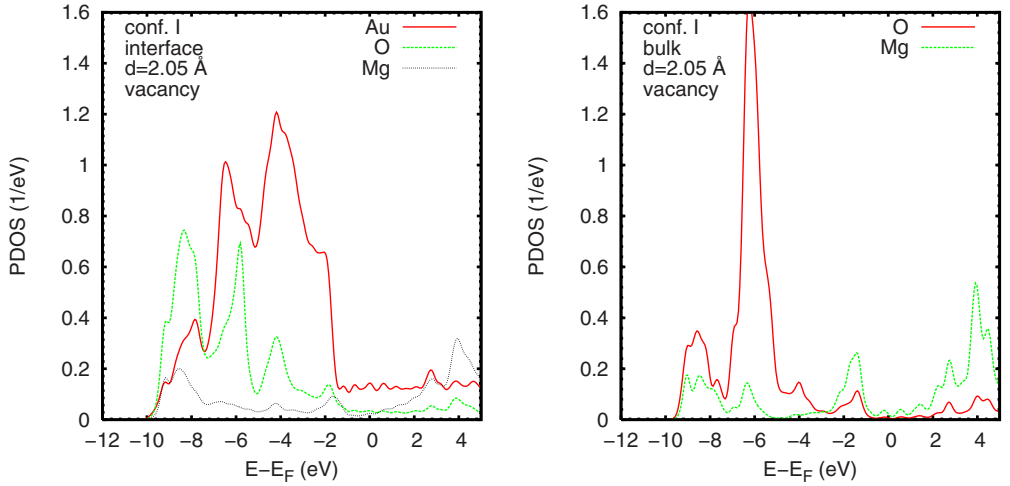

FIG. 8. (Color online) Projected DOS of atoms at the interface (left-hand side) and in the center of the MgO interlayer (right-hand side) for $n=1$ and a symmetric vacancy, where $d=2.05$ Å.

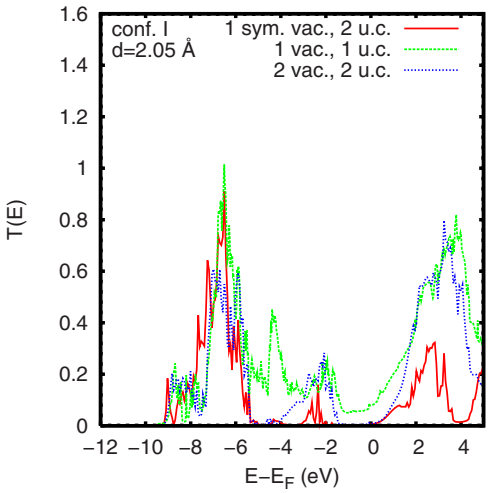

FIG. 9. (Color online) Comparison of the transmission coefficient for $n=1$ and $n=2$.

etrate into the center of thicker MgO interlayers, the transmission at the Fermi energy is drastically reduced in these cases. The I-V characteristic thus shows a higher conductance for $n=1$ than for $n=2,3$; note the scaling factor of 0.2 in Fig. 3.

Turning to conf. II, see Fig. 4, no Au-MgO bond is established since hybridized states are missing in the PDOS. The Au induced gap states reappear around the Fermi energy and again a reduced band gap is found for the interface Mg states. The O PDOS of the central MgO layer is similar for $n=2$ and 3 but deviates slightly in the $n=1$ case. Moreover, with the interlayer thickness the Mg-O hybridization increases and the PDOS peaks become more pronounced. A minor shoulder due to the Au induced gap states is present at −1.8 eV for $n=1$ but disappears for the thicker MgO interlayers. Due to the weak coupling to the metal, the shape of $T(E)$ in Fig. 5 again resembles the PDOS of bulk MgO. We find that the conductance of the tunnel junction in conf. II is smaller than obtained for conf. I. With increasing thickness of the MgO interlayer, d_{MgO}, it decreases exponentially

$$G = T(E_F) \propto \exp(-d_{\mathrm{MgO}}/1.41\ \text{Å}),$$

see the logarithmic plot in Fig. 5.

In the next step, we study the influence of the interface spacing on the charge transport through the Au-MgO-Au junction. As an example, we consider conf. I for $n=1$. The left-hand side of Fig. 6 shows the PDOS for interface atoms at an interface spacing of $d=3.06$ Å. The data resemble the PDOS of conf. II at $d=2.05$ Å, see Fig. 4. In particular, there is no sign of Au-O bonding. Thus, an Au-MgO distance of some 3 Å is sufficient to fully suppress the Au-O bonding. The O PDOS of atoms in the central MgO layer at different interface spacings is compared on the right-hand side of Fig. 6. It has been found theoretically that the stable Au-MgO distance is $d=2.5$ Å.[17] In this case the PDOS turns out to be similar to both bulk MgO and conf. II at $d=2.05$ Å, see Fig. 4. The band width amounts to ~6 eV, while it is ~7 eV for the shorter spacing. As to be expected, it decreases further to ~5 eV for $d=3.06$ Å. The rigid band shift with growing interface spacing is connected to the fact that the interface becomes more and more surfacelike. Figure 7 addresses the transport at different interface spacings. Both the onset and the shape of $T(E)$ are determined by the corresponding PDOS, see the right-hand side of Fig. 6.

IV. EFFECTS OF O VACANCIES

The effect of vacancies is discussed subsequently for conf. I and an interface spacing of $d=2.05$ Å. We address the following configurations: a symmetric vacancy generated by removing an O atom from the center of the MgO interlayer, an asymmetric vacancy located at 1/4 of the MgO interlayer, a vacancy located right at the interface, and a situation with two vacancies located at 1/4 and 3/4 of the MgO interlayer.

For the $n=1$ Au-MgO-Au junction and a symmetric vacancy the PDOS of the interface atoms is displayed on the left-hand side of Fig. 8. The main difference as compared to the clean system, see Fig. 2, is the appearance of vacancy induced Mg states in the energy range between −2.4 and

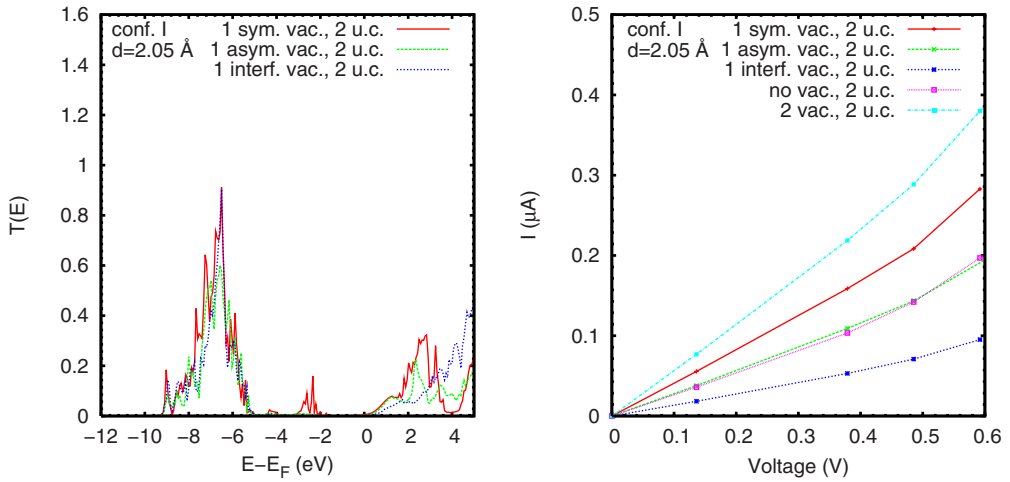

FIG. 10. (Color online) Transmission coefficient (left-hand side) and I-V characteristic (right-hand side) for $n=2$ and various vacancy configurations.

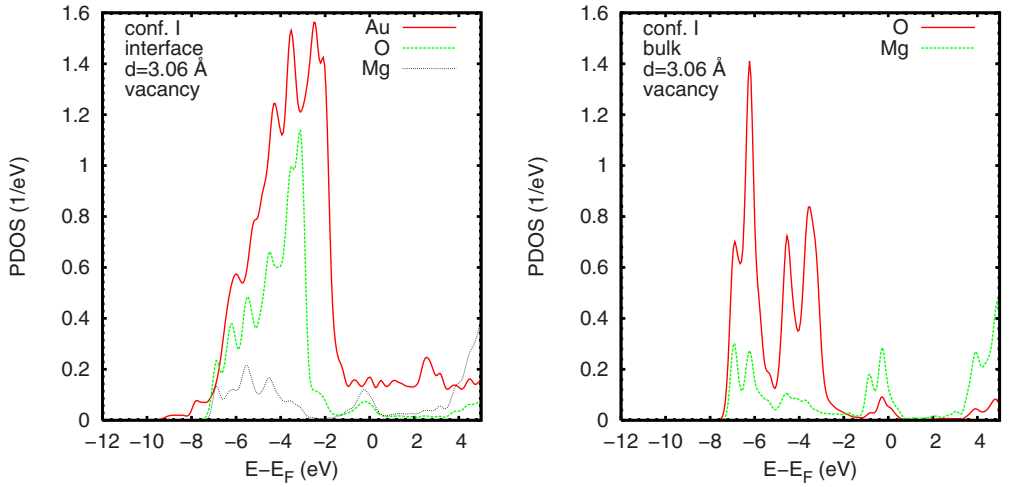

FIG. 11. (Color online) Projected DOS of atoms at the interface (left-hand side) and in the center of the MgO interlayer (right-hand side) for $n=1$ and a symmetric vacancy, where $d=3.06$ Å.

−0.4 eV. Therefore, the energy gap in the Mg states has vanished. Since the vacancy induced Mg states and the Au induced gap states are located in the same energy range they are difficult to separate. Therefore, we show on the right-hand side of Fig. 8 the PDOS of atoms in the central MgO layer. The vacancy induced Mg states are clearly visible.

As compared to the clean system, the transmission of the $n=2$ Au-MgO-Au junction can be enhanced by incorporating a symmetric vacancy, compare Fig. 9 to Fig. 3. This fact traces back to the vacancy states centered at about −2.5 eV. In the case of the $n=1$ Au-MgO-Au junction, the contribution of these states is even higher. According to Fig. 9, further enhancement of $T(E)$ can be achieved by incorporating asecond vacancy. In Fig. 10 we compare $T(E)$ findings and I-V characteristics of various vacancy configurations for the $n=2$ Au-MgO-Au junction. We observe that the transmission at the Fermi level decreases when the vacancy approaches the interface. Therefore, a symmetric vacancy enhances the conductance, whereas an asymmetric vacancy has almost no effect as compared to the clean system. Finally, the conductance is reduced for the interface vacancy, which represents the experimental case as vacancies accumulate at the interface. Confirming the above discussion, the largest conductance is found when a second vacancy is present. Therefore, enhancement of the transmission depends both on the number and the position of the vacancies. Finally, we investigate the influence of the interface spacing in O-deficient systems. Corresponding PDOS data for atoms at the interface and in the central MgO layer are displayed in Fig. 11. Interestingly, the vacancy induced Mg states now are located close to the Fermi energy, which further enhances the conductance.

V. CONCLUSION

In conclusion, we have studied the charge transport through Au-MgO-Au tunnel junctions using the SMEAGOL package. In particular, we have investigated the influence of the thickness of the MgO interlayer, the interface termination, and the interface spacing. An exponential decay of the conductance as a function of the interlayer thickness (as expected for tunnel junctions) is found only when Au-O bonds are missing, since such interface states enhance the conductance of ultrathin interlayers. An increasing interface spacing suppresses the Au-O bonding and the transmission becomes independent of structural details. The Au induced gap states are found to be similar in both terminations. The conductance decreases strongly with the interface spacing, since the Au-MgO coupling becomes weaker. The latter is reflected by a rigid band shift of the MgO states toward the Fermi energy.

Our results confirm that O vacancies can lead to additional states in the MgO band gap and, consequently, can enhance the conductance of the junction. The effects of symmetric vacancies turn out to be much larger than found for asymmetric vacancies. In addition, the conductance can be enhanced by increasing the vacancy concentration. In contrast to a clean junction where growing interface spacing always yields a reduction in the conductance, the rigid band shift of the MgO states here transfers the vacancy induced Mg states to the Fermi energy, which can be used to enhance the conductance in O-deficient systems. As a consequence, we have identified two main mechanisms which determine the conductance of Au-MgO-Au junctions: Introduction of O vacancies increases the transparency of the MgO interlayer due to the creation of additional electronic states close to the Fermi energy. The interface coupling then can be used to fine tune these states and, therefore, to fine-tune the conductance. Although the interface coupling is a very efficient parameter, it is difficult to control in an experiment.

ACKNOWLEDGMENT

We gratefully acknowledge discussions with P. Schwab and S. Sanvito. We thank the Deutsche Forschungsgemeinschaft (Grant No. SFB 484) and the Egyptian Missions System for financial support. The SMEAGOL project is sponsored by the Science Foundation of Ireland.

[1] M. W. Finnis, J. Phys.: Condens. Matter **8**, 5811 (1996).
[2] U. Schwingenschlögl and C. Schuster, Europhys. Lett. **81**, 17007 (2008); Chem. Phys. Lett. **467**, 354 (2009).
[3] U. Schwingenschlögl and C. Schuster, Europhys. Lett. **77**, 37007 (2007); Phys. Rev. Lett. **102**, 227002 (2009).
[4] B. Herschend, K. Hermansson, M. Alfredsson, Y. F. Zhukovsk III, E. A. Kotomin, and P. W. M. Jacobs, J. Phys. Chem. B **107**, 11893 (2003).
[5] A. Zaoui, Phys. Rev. B **69**, 115403 (2004).
[6] B. Meyer and D. Marx, Phys. Rev. B **69**, 235420 (2004).
[7] Zheshuai Lin and Paul D. Bristowe, Phys. Rev. B **75**, 205423 (2007).
[8] I. G. Batirev, A. Alavi, M. W. Finnis, and T. Deutsch, Phys. Rev. Lett. **82**, 1510 (1999).
[9] J. I. Beltrán, S. Gallego, J. Cerdá, J. S. Moya, and M. C. Munoz, Phys. Rev. B **68**, 075401 (2003).
[10] A. Markovits, J. C. Paniagua, N. López, C. Minot, and F. Illas, Phys. Rev. B **67**, 115417 (2003).
[11] J. Goniakowski, Phys. Rev. B **58**, 1189 (1998).
[12] S. A. Wolf, D. D. Awschalom, R. A. Buhrman, J. M. Daughton, S. von Molnar, M. L. Roukes, A. Y. Chtchelkanova, and D. M. Treger, Science **294**, 1488 (2001).
[13] I. Rungger, O. Mryasov, and S. Sanvito, Phys. Rev. B **79**, 094414 (2009).
[14] H. B. Groen, B. J. Kooi, W. P. Vellinga, and J. Th. M. De Hosson, Philos. Mag. A **79**, 2083 (1999).
[15] D. K. Chan, D. N. Seidman, and K. L. Merkle, Phys. Rev. Lett. **75**, 1118 (1995).
[16] D. A. Muller, D. A. Shashkov, R. Benedek, L. H. Yang, J. Silcox, and D. N. Seidman, Phys. Rev. Lett. **80**, 4741 (1998).
[17] D. Chen, X. L. Ma, and Y. M. Wang, Phys. Rev. B **75**, 125409 (2007).
[18] J. Goniakowski and C. Noguera, Interface Sci. **12**, 93 (2004).
[19] Q. S. Wang and N. A. W. Holzwarth, Phys. Rev. B **41**, 3211 (1990).
[20] L. A. Kappers, R. L. Kroes, and E. B. Hensley, Phys. Rev. B **1**, 4151 (1970).
[21] J. Xu, A. P. Mills, Jr., A. Ueda, D. O. Henderson, R. Suzuki, and S. Ishibashi, Phys. Rev. Lett. **83**, 4586 (1999).
[22] C. Barth and C. R. Henry, Phys. Rev. Lett. **91**, 196102 (2003).
[23] K. Honkala and H. Häkkinen, J. Phys. Chem. C **111**, 4319 (2007).
[24] J. P. Velev, K. D. Belashchenko, S. S. Jaswal, and E. Y. Tsymbal, Appl. Phys. Lett. **90**, 072502 (2007).
[25] J. M. Soler, E. Artacho, J. D. Gale, A. García, J. Junquera, P. Ordejón, and D. Sánchez-Portal, J. Phys.: Condens. Matter **14**, 2745 (2002).
[26] A. R. Rocha, V. M. Garcia-Suarez, S. W. Bailey, C. J. Lambert, J. Ferrer, and S. Sanvito, Nature Mater. **4**, 335 (2005); Phys. Rev. B **73**, 085414 (2006).
[27] I. Rungger and S. Sanvito, Phys. Rev. B **78**, 035407 (2008).
[28] M. Fadlallah, C. Schuster, U. Schwingenschlögl, T. Wunderlich, and S. Sanvito, J. Phys.: Condens. Matter **21**, 315001 (2009).
[29] L. Kleinman and D. M. Bylander, Phys. Rev. Lett. **48**, 1425 (1982).
[30] Z. Yang, R. Wu, Q. Zhang, and D. W. Goodman, Phys. Rev. B **65**, 155407 (2002).
[31] J. Peralta-Ramos, A. M. Llois, I. Rungger, and S. Sanvito, Phys. Rev. B **78**, 024430 (2008).
[32] H. Baltache, R. Khenata, M. Sahnoun, M. Driz, B. Abbar, and B. Bouhafs, Physica B **344**, 334 (2004).
[33] M. Klaua, D. Ullmann, J. Barthel, W. Wulfhekel, J. Kirschner, R. Urban, T. L. Monchesky, A. Enders, J. F. Cochran, and B. Heinrich, Phys. Rev. B **64**, 134411 (2001).
[34] J. Goniakowski, Phys. Rev. B **57**, 1935 (1998).